

### Supporting Information

Synthesis of graphene-like CuB<sub>23</sub> nanosheets with fast and stable response to H<sub>2</sub>S at ppb level detection

Ming Ming Chen,<sup>a,b#</sup> Chu Lin Huang,<sup>a,b#</sup> Wei Chu,<sup>c</sup> Li Ping Hou<sup>a,b</sup> and Dong Ge Tong<sup>\*a,b</sup>

<sup>a</sup> State Key Laboratory of Geohazard Prevention and Geoenvironment Protection (Chengdu University of Technology), Chengdu 610059, China.

<sup>b</sup> Collaborative Innovation Center of Panxi Strategic Mineral Resources Multi-purpose Utilization, College of Materials and Chemistry & Chemical Engineering, Chengdu University of Technology, Chengdu 610059, China. E-mail: tongdongge@163.com; Fax: +86 28 8407 8940

<sup>c</sup> College of Chemical Engineering and Key Laboratory of Green Chemistry & Technology of Ministry of Education, Sichuan University, Chengdu 610065, China.

# These authors contributed equally

Summary: 17 Pages; 12 Figures; 1 Table

## Table of Contents

Experimental.....	3
Preparation of graphene-like CuB <sub>23</sub> .....	3
Characterization.....	3
Manufacture and Testing of Gas Sensor .....	4
Table S1 .....	5
Fig.S1 .....	6
Fig.S2 .....	7
Fig.S3 .....	8
Fig.S4 .....	9
Fig.S5 .....	10
Fig.S6 .....	11
Fig.S7 .....	12
Fig.S8 .....	13
Fig.S9 .....	14
Fig.S10 .....	15
Fig.S11 .....	16
Fig.S12 .....	17

## 1. Experimental

### 1.1. Preparation of graphene-like CuB<sub>23</sub>

The self-designed SPT reactor used for the preparation of graphene-like CuB<sub>23</sub> was present in our previous study.<sup>51</sup> The pulsed direct current voltage was 200 V (duty: 90%, frequency: 12 kHz). The electrodes were tungsten wire (diameter: 2 mm) and the gap between the cathode and anode was 1 mm.

In a typical synthesis, 40 mL of 25% NH<sub>3</sub>·H<sub>2</sub>O solution was mixed with 10mL of copper chloride (0.0085 mol) to form a Cu(NH<sub>3</sub>)<sub>6</sub><sup>2+</sup> complex. Then 32 mL of 1.0 M KBH<sub>4</sub> aqueous solution, and 0.010 M PVA (Mw = 10000) was added at 298 K under an argon atmosphere. The SPT was carried out for 15 min. The obtained product was washed with deionized water, followed by three washings with alcohol. Finally, the sample was dried at 60 °C. The commercial CuB<sub>23</sub> samples were provided by the Changzhen High Technology Limited Company.

### 2.2. Characterization

X-ray diffraction (XRD) patterns were recorded using an X'Pert X-ray powder diffractometer equipped with a CuK $\alpha$  radiation source ( $\lambda = 0.15406$  nm). The Cu and B contents in the samples were determined by inductively coupled plasma atomic emission spectroscopy (ICP-AES; Iris, Advantage). The Brunauer–Emmett–Teller (BET) specific surface area of the sample was made using a N<sub>2</sub> adsorption–desorption technique. Before the measurements, the sample was degassed at 473 K for 3 h. Scanning transmission electron microscopy (STEM) images and selected-area electron diffraction patterns (SAED) of the samples were carried out with a JEOL-2100F microscope. Samples for STEM analysis were fabricated by depositing a single drop of diluted nanoparticle dispersion in ethanol on an amorphous, carbon-coated, nickel grid. The surface electronic states of the samples were determined using X-ray photoelectron spectroscopy (XPS; Perkin–Elmer PHI 5000C ESCA, using AlK $\alpha$  radiation). Samples were fixed in a homemade in situ XPS reactor cell.<sup>44,45,49</sup> After the samples were dried under an argon atmosphere, they were transferred to an analysis chamber, and their XPS spectra were recorded. All binding

energies were referenced to the C1s peak (binding energy of 284.6 eV) of the surface adventitious carbon. Infrared spectra were acquired using a Bruker FTIR spectrometer (EQUINOX55). The emission spectra of SPT, temperature distribution and electron concentration variation in the envelope were obtained by AvaSpec-3648 optical fiber apparatus controlled with a Matlab software. The AFM image of the sample deposited on the silicon wafer substrate was obtained by atomic force microscope (Veeco D3100, USA) under the conditions of relative humidity of 63% at 20 °C with a tapping mode at a 1-3Hz scan rate and a 512×512 pixel resolution.

### **2.3. Manufacture and Testing of Gas Sensor**

The gas sensing test was performed in an HW-30A measuring system (Hanwei Electronics Co. Ltd.) controlled with a Lab-VIEW software at room temperature under 60% relative humidity (RH). For measuring, the sample was mixed with terpineol to form a paste and then coated onto a commercial Interdigitated Electrode (IDE) to fabricate a capacitive sensor. The IDE has a silicon wafer depositing layers of 2 μm electrical isolation oxide and 10 nm Ti and 300 nm Au, and is patterned with conventional photolithography process. A pair of Au wires was annealed to perform the electrical measurements. During assessing, argon is used as a carrier gas to dilute the H<sub>2</sub>S to desired concentration. Their concentrations of H<sub>2</sub>S and argon are monitored by mass flow controllers. Moreover, we have also investigated the water-sensing response of graphene-like CuB<sub>23</sub> nanosheets exposing to different RH water vapor. The H<sub>2</sub>S gas sensing performances of our sample under 30%RH and 80%RH were also evaluated. The detection limits in both ppm and ppb levels of H<sub>2</sub>S were calculated based on the root-mean-square deviation method.

**Table S1** Specific surface areas of different CuB<sub>23</sub> samples

Samples	Specific surface areas / m <sup>2</sup> g <sup>-1</sup>
CuB <sub>23</sub> nanotubes <sup>24</sup>	84.7
CuB <sub>23</sub> /graphene <sup>25</sup>	133.2
commercial CuB <sub>23</sub>	28.2
Graphene-like CuB <sub>23</sub> nanosheets in this work	674.9
CuB <sub>23</sub> NPs prepared by SPT for 1 min in this work	32.4
CuB <sub>23</sub> NPs prepared by SPT for 5 min in this work	50.8
CuB <sub>23</sub> NPs prepared by SPT for 10 min in this work	73.3

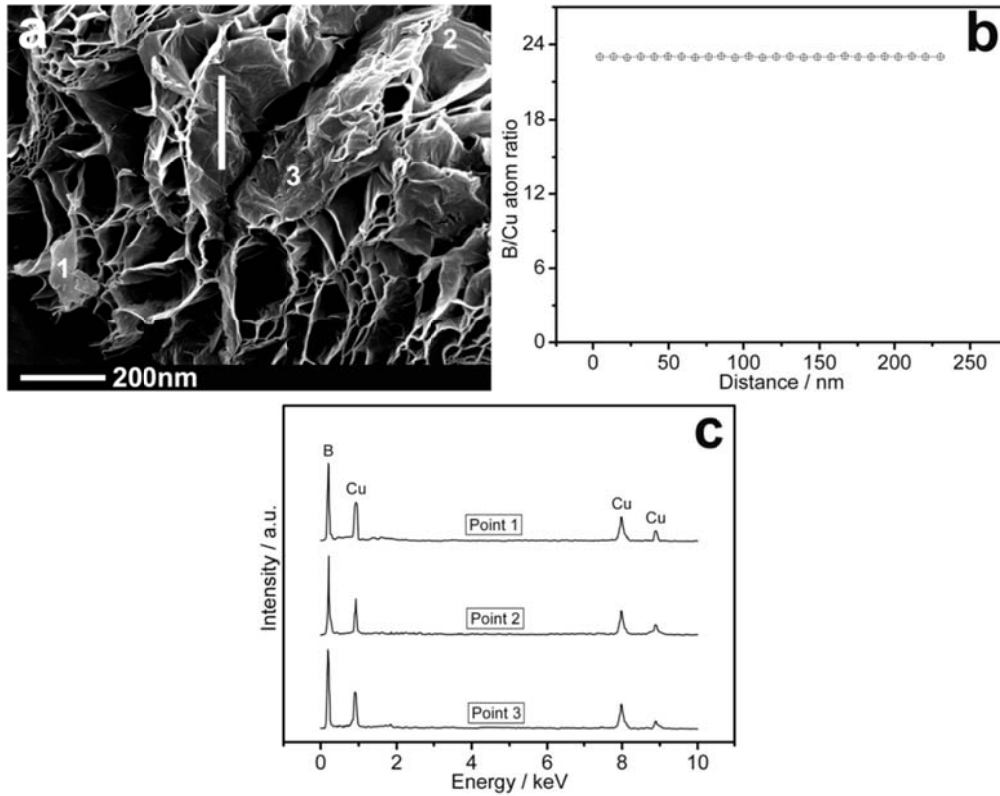


**Fig.S1** (a) The high-angle annular dark-field scanning transmission electron microscopy (HAADF-STEM); (b) B/Cu atomic ratio recorded along the white cross-sectional compositional line shown in (a); (c) the Energy-dispersive X-ray spectroscopy (EDAX) at points 1-3 in (a) of the as-prepared graphene-like amorphous  $\text{CuB}_{23}$  alloy nanosheets

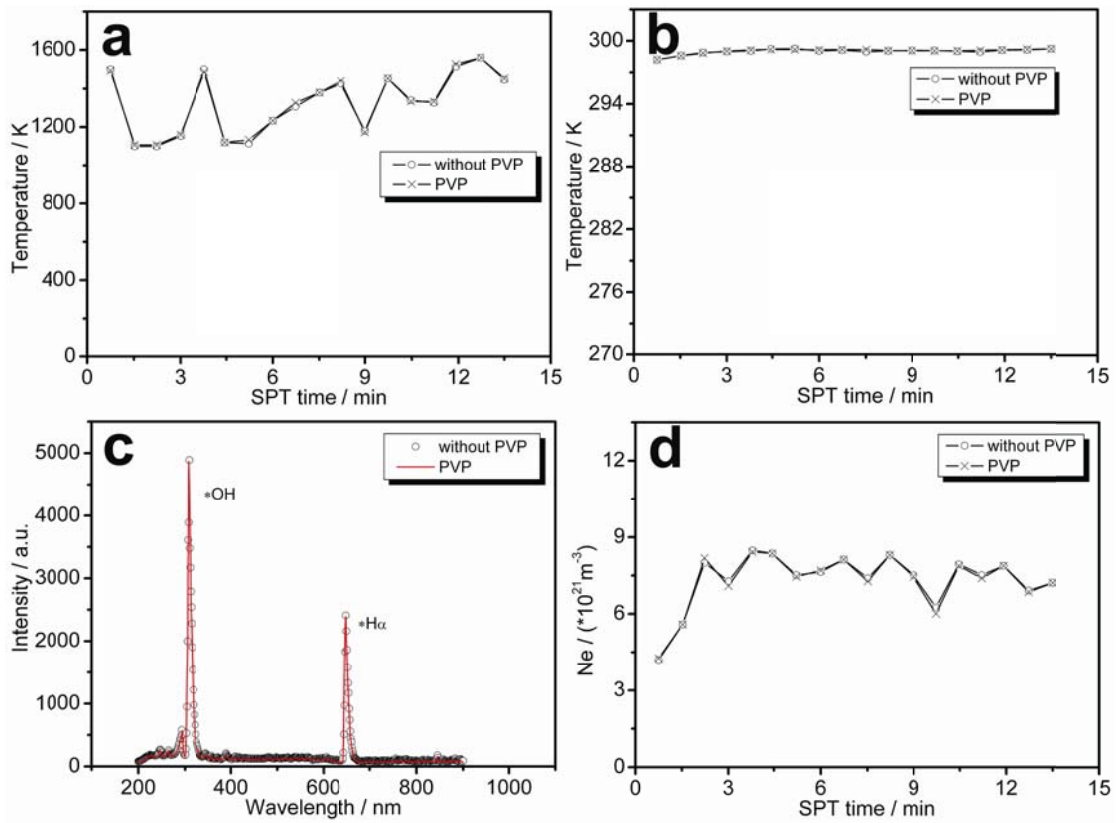


**Fig.S2** (a) Electron temperature variation with discharge time; (b) Solution temperature variation with discharge time; (c) The emission spectra of SPT; (d) Electron concentration variation with SPT time with the addition of 0.010 M PVP or not

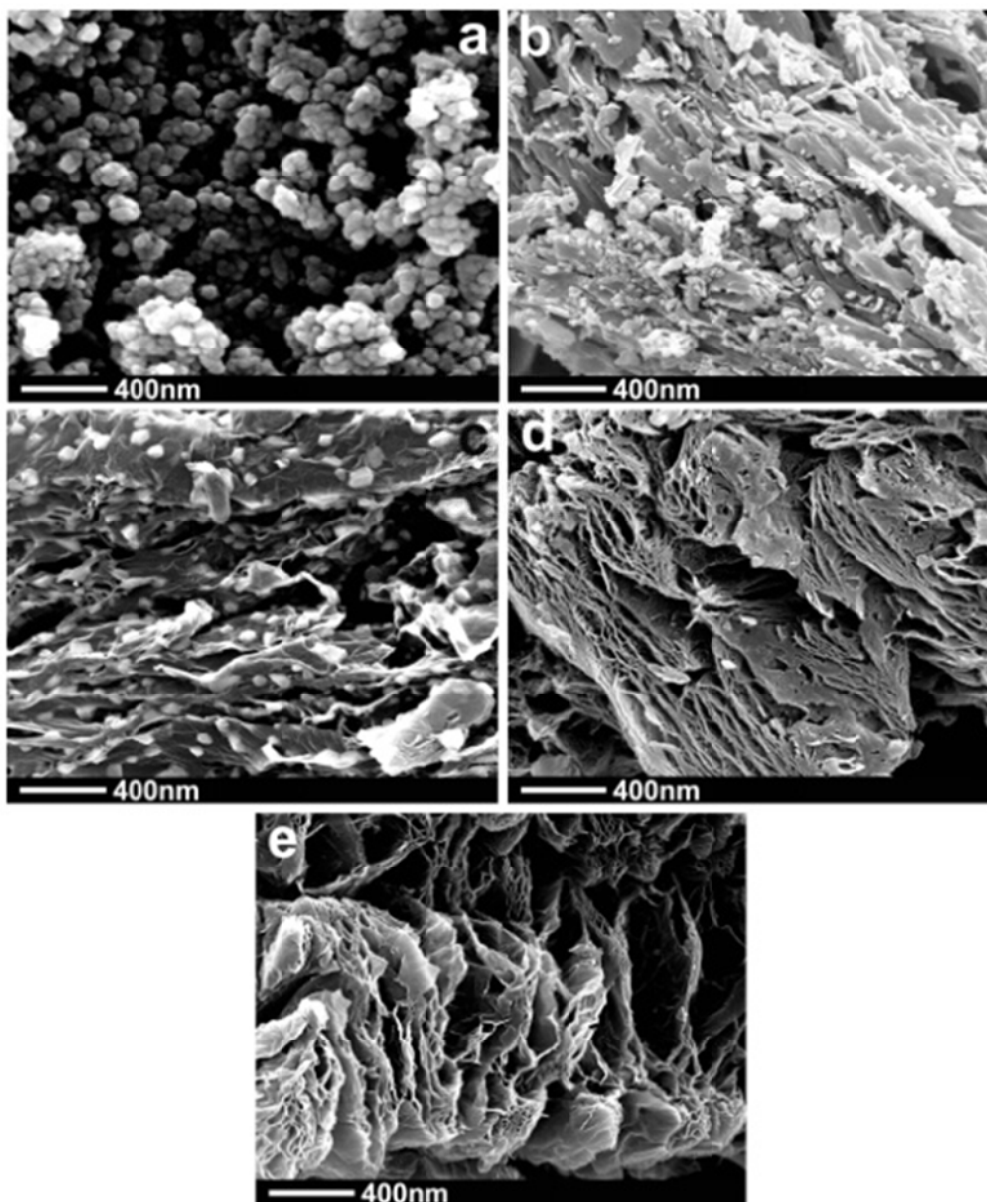


**Fig.S3** STEM images of the graphene-like amorphous CuB<sub>23</sub> alloy nanosheets prepared by SPT with different concentrations of PVP (a) 0; (b) 0.002; (c) 0.005; (d) 0.010 M; (e) 0.015 M



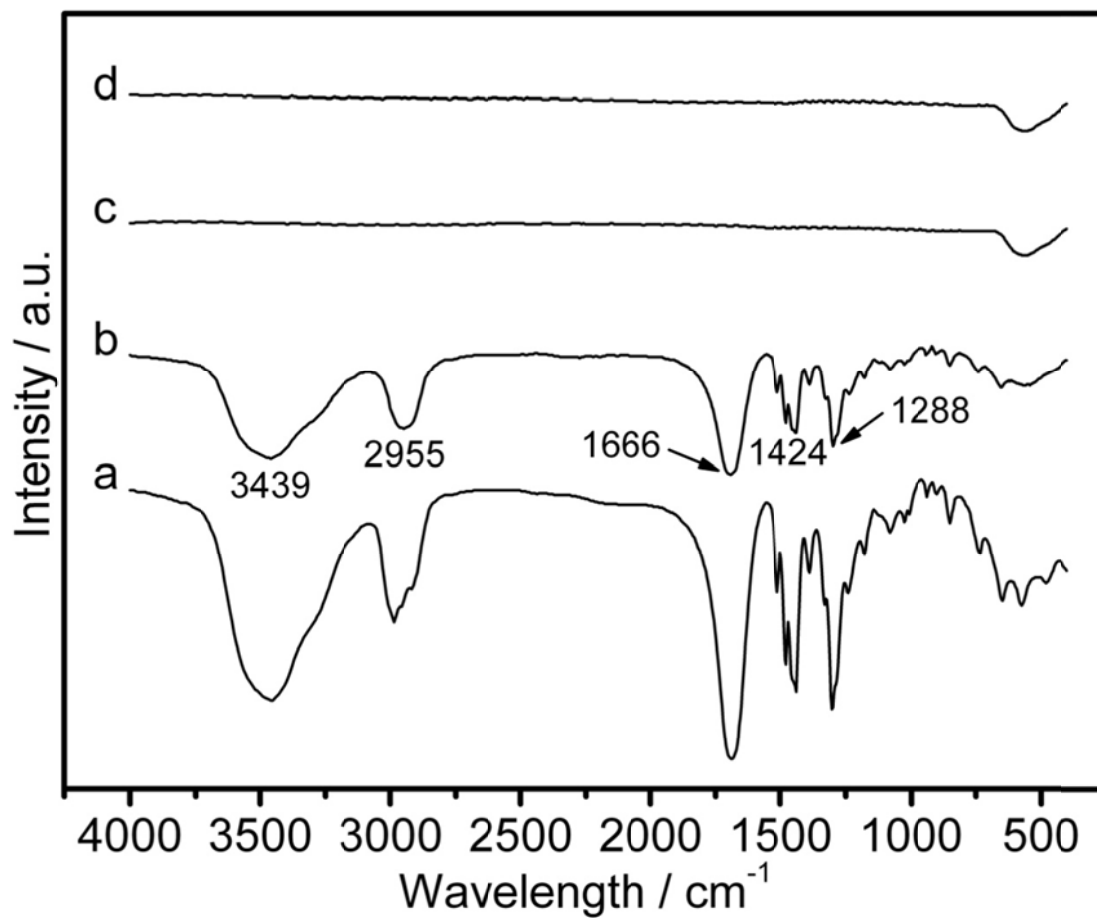


**Fig.S4** FT-IR spectra of (a) PVP; (b) the as-prepared graphene-like amorphous  $\text{CuB}_{23}$  alloy nanosheets only washed with water; (c) the as-prepared graphene-like amorphous  $\text{CuB}_{23}$  alloy nanosheets washed with ethanol; and (d) commercial  $\text{CuB}_{23}$  NPs

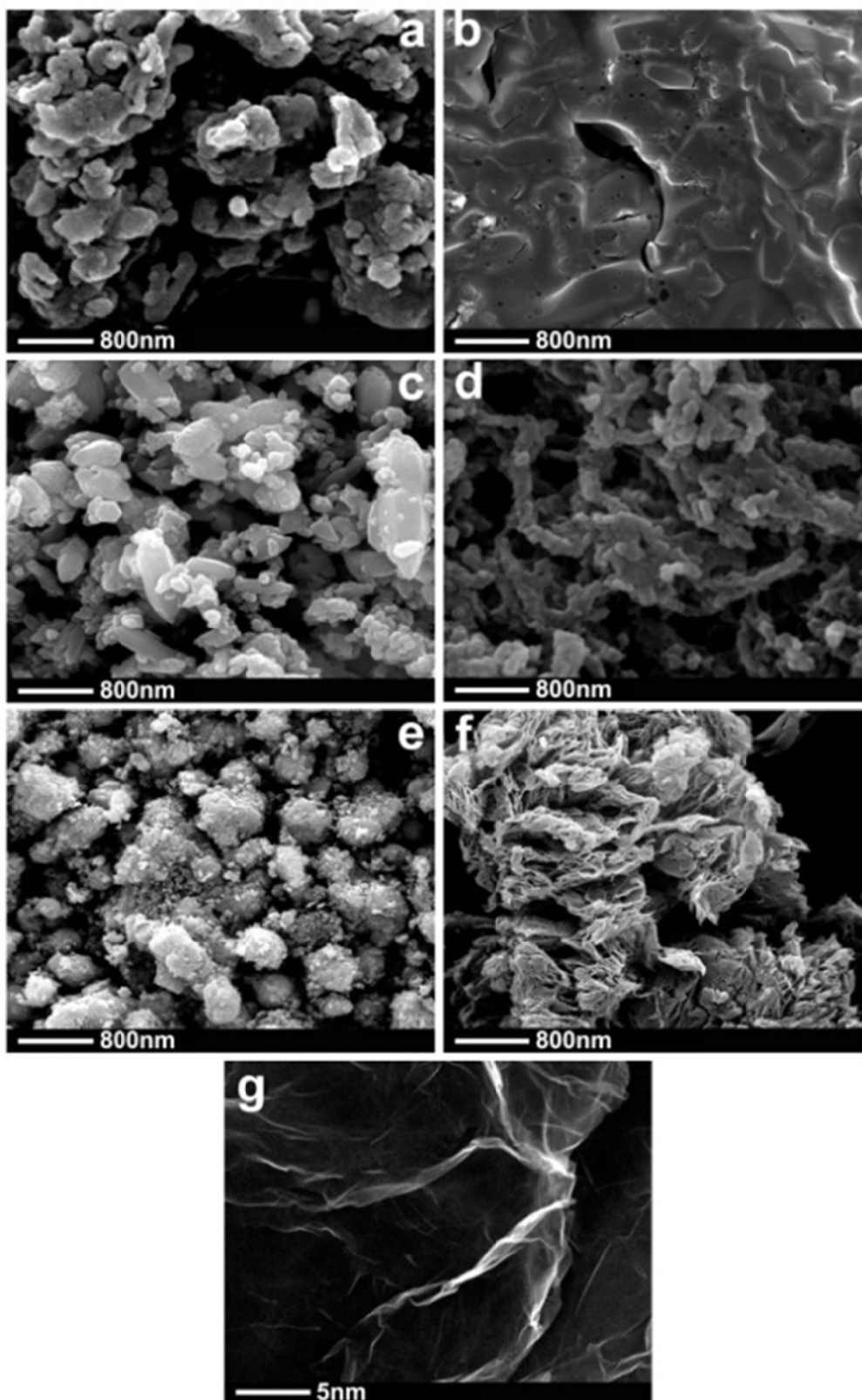


**Fig.S5** STEM images of the graphene-like amorphous  $\text{CuB}_{23}$  alloy nanosheets prepared by SPT with (a) CTAB; (b) PVA; (c) P123; (d) ethylenediamine; (e) SDBS; (f, g) either of (a)-(e) after additional of PVP at different magnifications

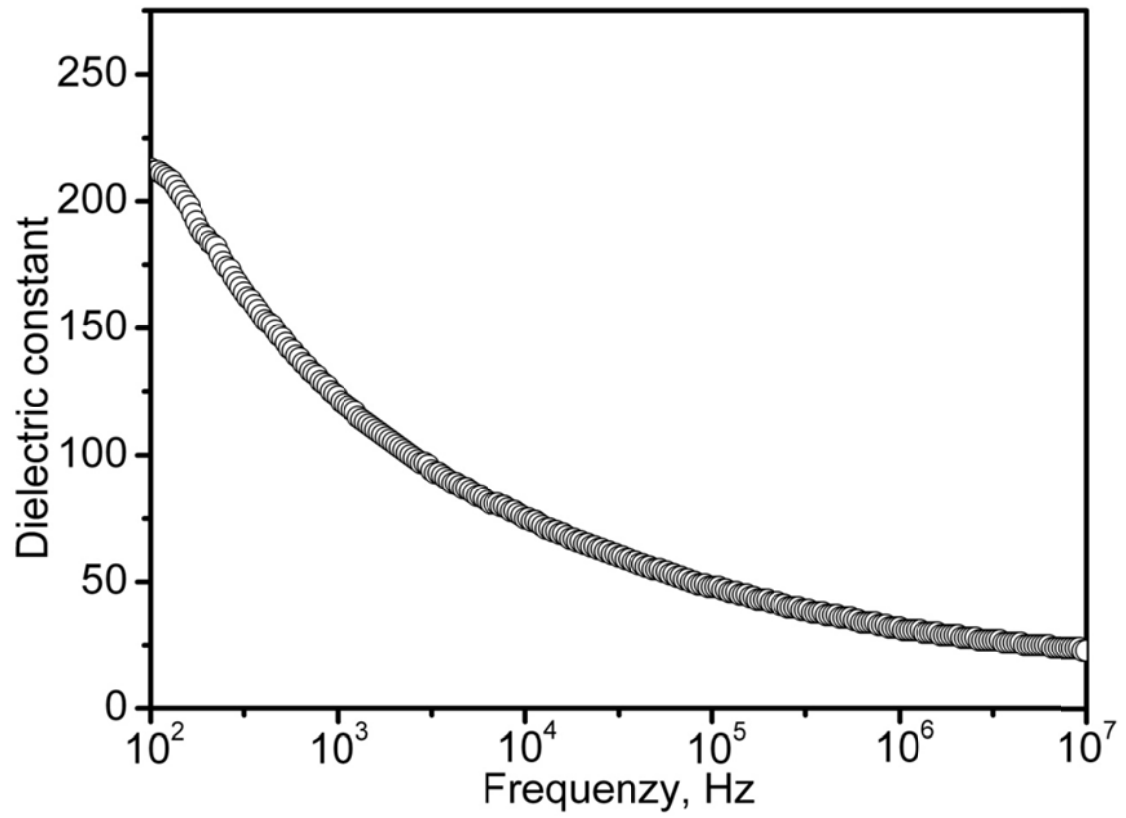


**Fig.S6** Measured dielectric constant of the graphene-like amorphous  $\text{CuB}_{23}$  alloy nanosheets from  $10^2$  Hz to  $10^7$  Hz

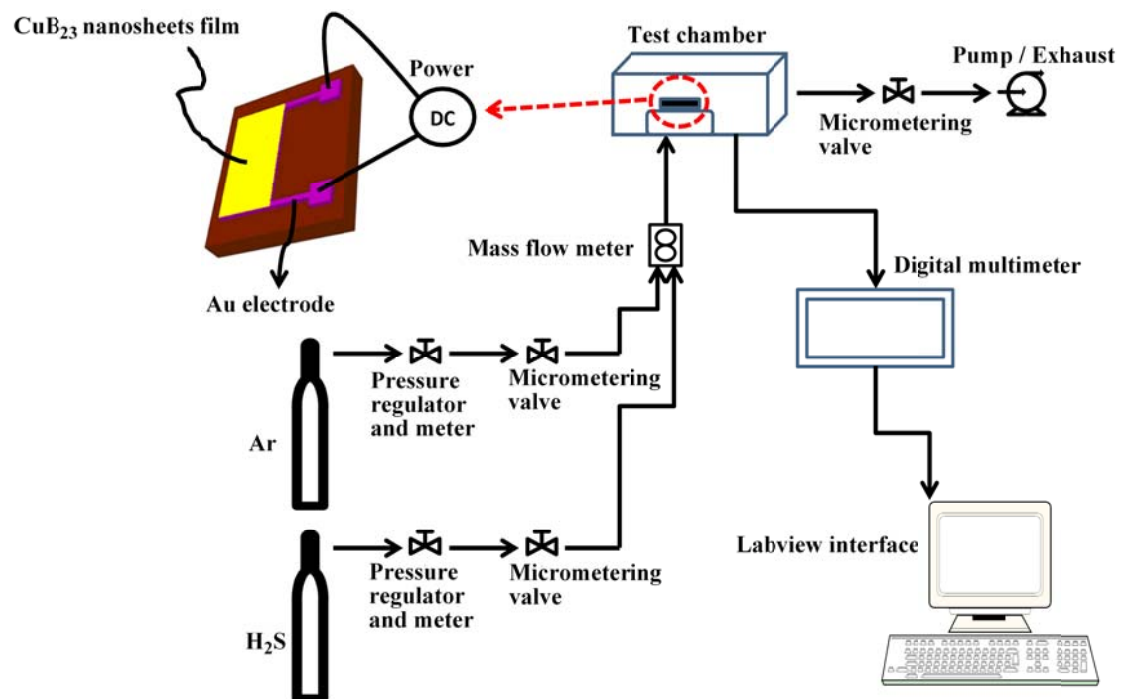


**Fig.S7** Schematic diagram of the sensor measurement system with magnified sensor device configuration in our work

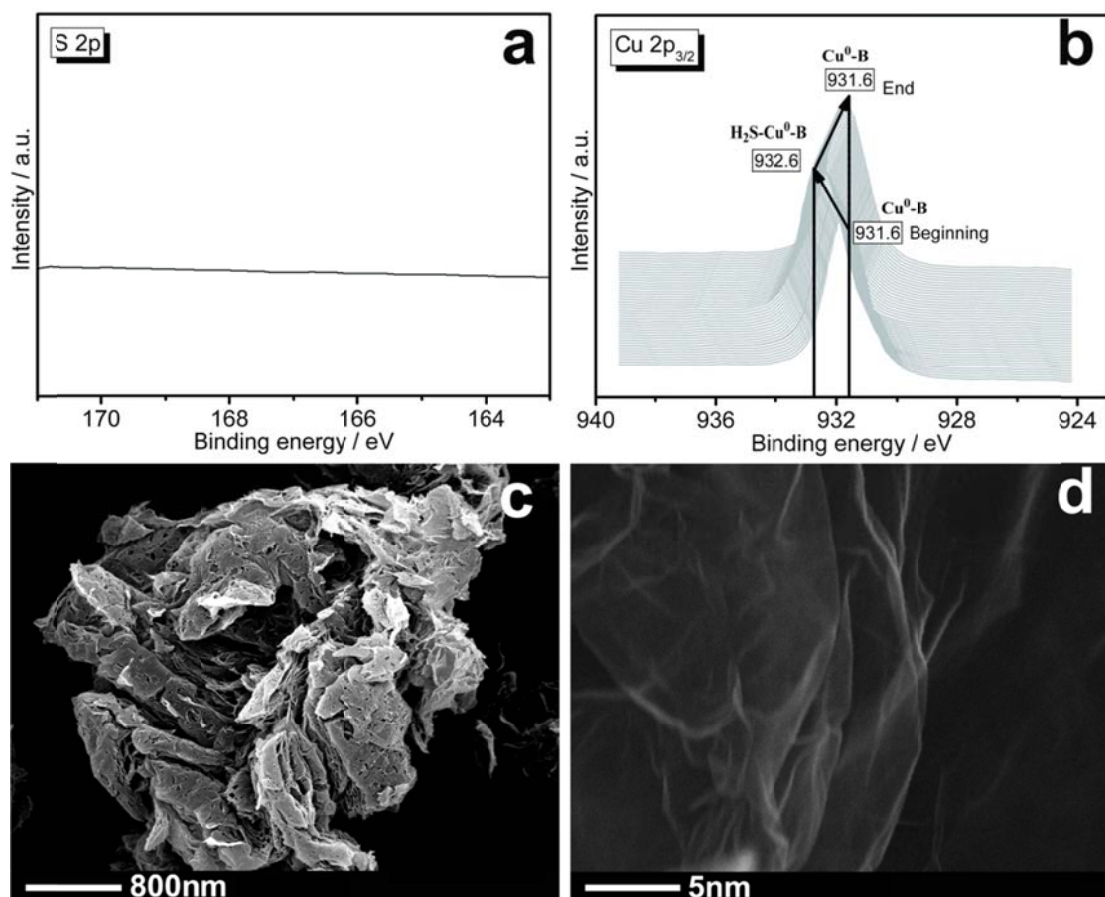


**Fig.S8** (a) S 2p XPS spectrum of the graphene-like amorphous CuB<sub>23</sub> alloy nanosheets after exposure to H<sub>2</sub>S; (b) In-situ Cu 2p<sub>3/2</sub> spectra of the graphene-like amorphous CuB<sub>23</sub> alloy nanosheets during detection of H<sub>2</sub>S; (c, d) STEM images of the recycled the graphene-like amorphous CuB<sub>23</sub> alloy nanosheets after 6 months testing at different magnifications

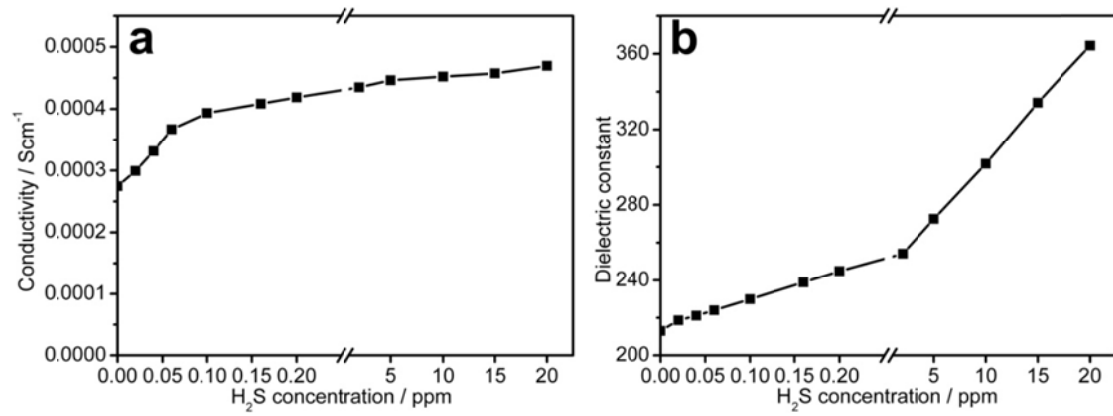


**Fig.9** Variation of (a) conductivity and (b) dielectric constant (at 100 Hz) of the graphene-like amorphous CuB<sub>23</sub> alloy nanosheets at different H<sub>2</sub>S gas concentrations from 20 ppb to 20 ppm

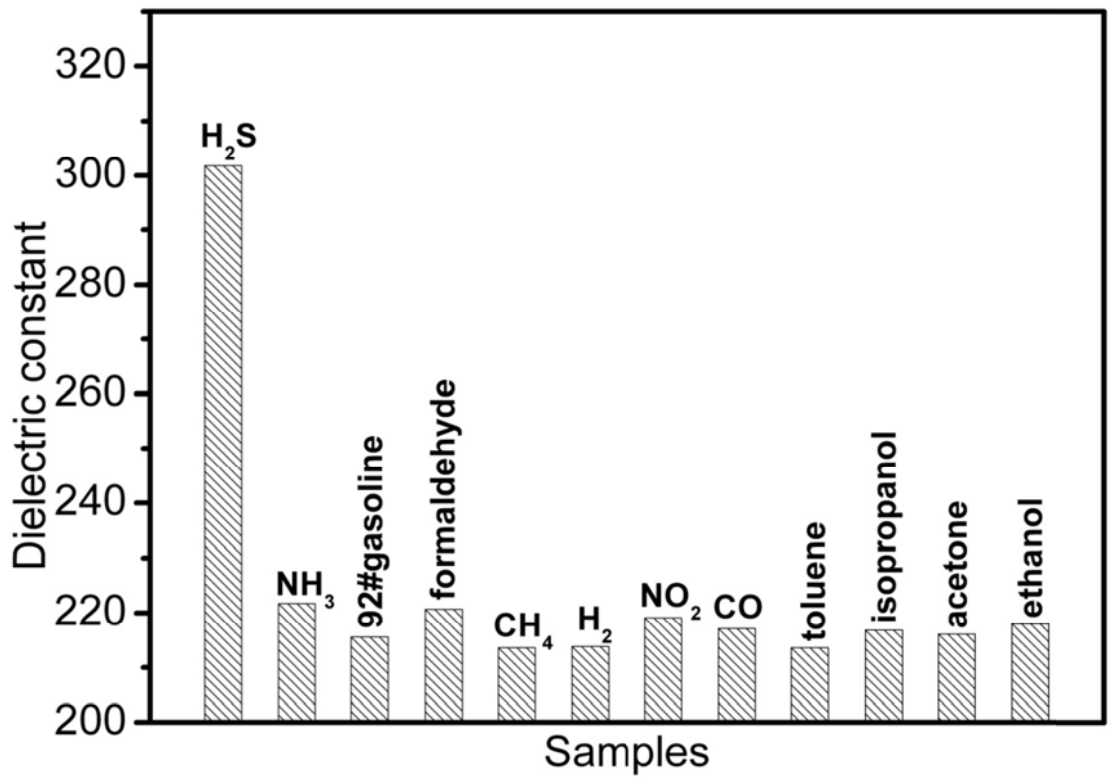


**Fig.10** The measured dielectric constant (at 100 Hz) of the graphene-like amorphous CuB<sub>23</sub> alloy nanosheets under 10 ppm different gases

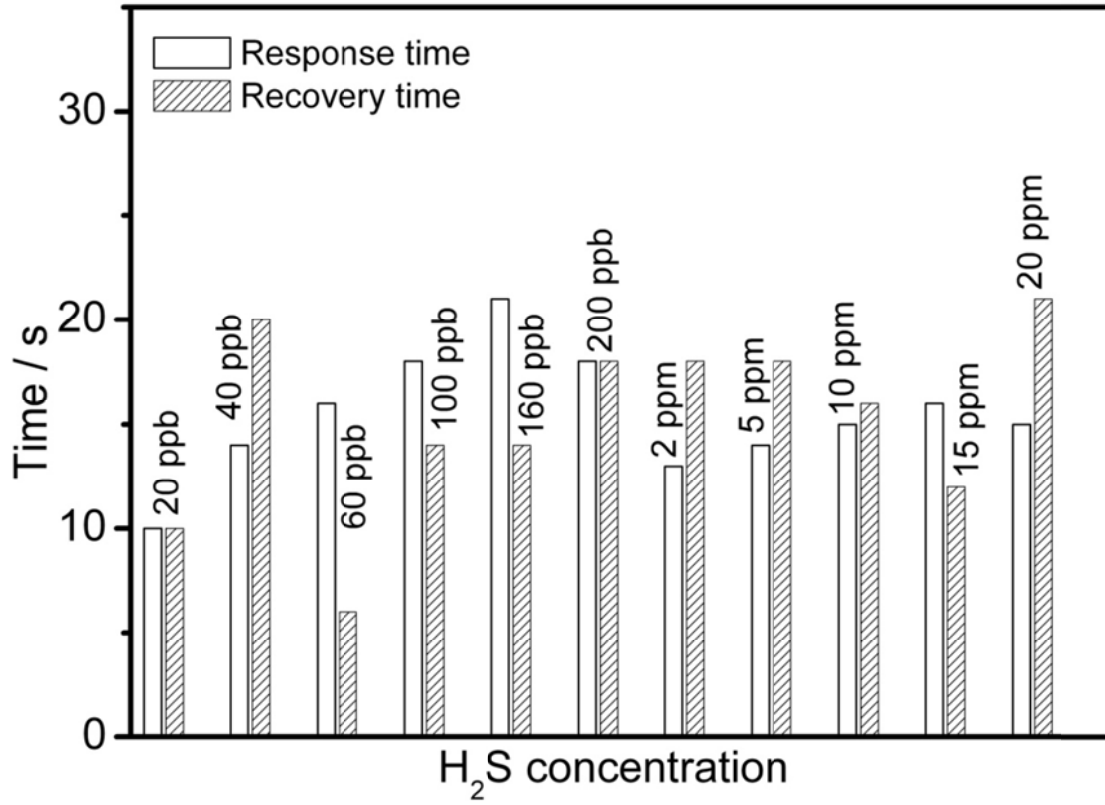


**Fig.S11** Variation of response time and recovery time of the graphene-like amorphous CuB<sub>23</sub> alloy nanosheets at different H<sub>2</sub>S gas concentrations from 20 ppb to 20 ppm



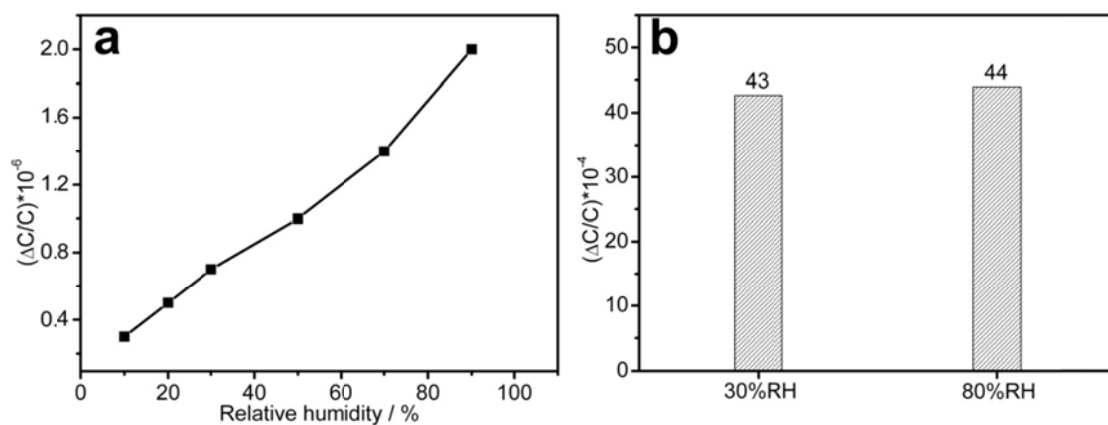


**Fig.S12** Response of the graphene-like amorphous CuB<sub>23</sub> alloy nanosheets (a) to different related humidity (RH) water vapor and (b) to H<sub>2</sub>S at 30% RH and 80% RH, respectively